Received: 25 January 2023 | Revised: 4 April 2023 | Accepted: 11 April 2023

DOI: 10.1002/ar.25230

RESEARCH ARTICLE

The Anatomical Record WILEY

Anatomy and computed tomography of the nasal cavity, nasal conchae, and paranasal sinuses of the endangered Patagonian huemul deer (*Hippocamelus bisulcus*)

Samuel Núñez-Cook[1,2] | **Fernando Vidal-Mugica**[3,4,5,6] | **Paulo Salinas**[1]

[1]Laboratory of Animal & Experimental Morphology, Institute of Biology, Faculty of Sciences, Pontificia Universidad Católica de Valparaíso, Valparaíso, Chile

[2]MSc Program in Morphological Sciences, Universidad de La Frontera, Temuco, Chile

[3]Departamento de Ciencias Básicas, Facultad de Ciencias, Universidad Santo Tomas, Temuco, Chile

[4]Fauna Andina, Wildlife Conservation and Management Center, Villarrica, Chile

[5]IUCN, Deer Specialist Group, Apple Valley, Minnesota, USA

[6]IUCN, Conservation Planning Specialist Group, Apple Valley, Minnesota, USA

Correspondence
Paulo Salinas, Laboratory of Animal & Experimental Morphology, Institute of Biology, Faculty of Sciences, Pontificia Universidad Católica de Valparaíso, Valparaíso, Chile.
Email: paulo.salinas@pucv.cl

Funding information
Innovative Interdisciplinary Research, Grant/Award Number: PUCV-DI 039.407/2021

Abstract

This study explores for the first time the shape, volume, and configuration of nasal cavity structures of the endangered Patagonian huemul deer via computed tomography (CT). Three-dimensional (3D) reconstructions derived from data sets obtained from five Patagonian huemul deer skulls were analyzed. Using semiautomatic segmentation, 3D models were created of all the sinus compartments and nasal conchae. Volumetric measurements were taken of seven sinus compartments. The Patagonian huemul deer has a wide, large nasal cavity, with an osseous nasal aperture typical of cervids and a choana with characteristics that differentiate it from the pudu and roe deer. It also has six nasal meatuses and three nasal conchae, with the ventral nasal concha having the greatest volume and surface, which given its extension ensures a greater ability to humidify and heat the air. Further analysis showed the complex system of paranasal sinuses to be characterized by a rostroventral and interconnected group, where communication with the nasal cavity is common through the nasomaxillary opening, and a caudodorsal group that communicates with the nasal cavity through openings in the nasal meatuses. Our study of the endangered Patagonian huemul deer documents an intricate, and in some nasal cavity structures, unique morphological construction which may predispose it to higher rates of sinonasal afflictions due largely to its nasal complex anatomy, thus affecting its high cultural value.

KEYWORDS

3D reconstruction, computed tomography, deer, huemul, nasal cavity, paranasal sinuses

1 | INTRODUCTION

In tetrapods, the nasal cavity is large and generally includes extensive nasal conchae that guarantee that the air that enters becomes warm and moist before entering the lungs. In mammals, the paranasal sinuses are a complex bilateral system of cavities filled with air. The nasal cavity, the nasal conchae, and the paranasal sinuses make up an anatomical and functional unit that can be described as the *nasal complex*. Covered by the same mucosa, the paranasal sinuses communicate with the nasal cavity through openings that allow both the ventilation and drainage of the sinuses. These structures are considered the starting point of the respiratory system, and thus they constitute the access point for external pathogens. Márquez (2008) has compiled the various functional roles proposed for the paranasal sinuses of vertebrates, such as lightening the weight of the skull,

forming bony pillars for the dispersal of force, mechanical and thermal protection for the central nervous system, as well as related physiological roles related to olfactory mucosa, regulation of the conditions of the inspired air and even impart resonance to the voice.

From a clinical perspective, osteopathies, lymphadenitis, and chronic bone infections in cervids and production animals that live alongside the Patagonian huemul deer promote the need for a circumstantial improvement in *in vivo* diagnoses given the morbidity reported in clinical cases involving the head (Escobar Ruíz et al., 2020; Flueck, 2015, 2018, 2020; Flueck & Smith-Flueck, 2020; Llanos-Soto et al., 2020). Chronic bone infection is one of the most frequent pathologies responsible for causing sinusitis (Escobar Ruíz et al., 2020), and the surgical treatment in domestic species varies according to the anatomical formation of the paranasal sinuses (Boiani Fernández & Van Wassenhove Olascoaga, 2015). Accordingly, the clinical anatomy of the Patagonian huemul deer cannot be assumed nor be based on descriptions made previously for domestic species (Hofmann, 1989); in other words, taking actions based solely on these is inefficient and irresponsible. Despite the clinical importance and the presentation of diseases that involve the paranasal sinuses and nasal conchae in our deer study, little is known of its anatomy. In previous anatomical descriptions, we have reported differences in thickness between bones of the appendicular skeleton (Salinas, Arenas-Caro, et al., 2020; Salinas, Núñez-Cook, et al., 2020) and bones of the neurocranium (Núñez-Cook et al., 2022), suggesting a possible unequal nutritional food chain among the geographic locations inhabited by the individuals studied. Following from this study, what the morphological effect of nutritional deficiency has on the nasal cavity, nasal conchae and paranasal sinuses is currently unknown.

Due to the overlap of structures in the nasal chamber (e.g., convoluted nasal conchae), conventional radiology does not allow the precise exploration of the region, particularly of the communicating openings, closely related to the sinus physiopathology, and therefore interesting from the point of view of applied anatomy. Revolutionary changes in the surgical treatment of sinusitis in recent years, particularly in endonasal endoscopic surgery, associated with advances in the knowledge of anesthetic protocols in endangered wild species, require the surgeon to have precise knowledge of the anatomy of the paranasal sinuses and the large number of anatomical variants existing in the region (Fatterpekar et al., 2008). Therefore, understanding the anatomy of the nasal cavity, nasal conchae, and paranasal sinuses of the Patagonian huemul deer is fundamental to the biological understanding of a species declared endangered from a morphological perspective, as this will benefit conservation, surgical and clinical medicine. The objective of the study was to describe the nasal cavity (with emphasis on the nasoturbinal and maxilloturbinal regions), nasal conchae and paranasal sinuses of the endangered Patagonian huemul deer including a clinical and morphofunctional interpretation to serve as a reference for clinical use, biomedical research, and teaching purposes.

2 | MATERIALS AND METHODS

The study was conducted in the Laboratory of Animal and Experimental Morphology in the Institute of Biology of the Pontifical Catholic University of Valparaiso. A descriptive and cross-sectional design was used. Five ($n_{total} = 5$; Male = 4; Female = 1) skulls of Patagonian huemul deer obtained by exhumation in the Region of La Araucanía (Fauna Andina; Villarrica 39°16′00″S, 72°13′00″W; 227 m.a.s.l., Chile) and in the Region of Aysén del General Carlos Ibáñez del Campo (Lake Paloma 45°55′00.7″S 72°08′34.3″W and Cerro Castillo 46°03′00″S 72°11′00″O; Chile) were used. All the skulls studied were obtained legally under the Hunting Law n°19473 frame and the resolution n°1490 (December 22, 2003) of the Agricultural and Livestock Service of Chile (SAG). Some came from wild and others from captive breeding conservation projects. Causes of death of the specimens studied were parasites, caseous lymphadenitis, and intraspecific fights. One of the skulls was missing the dorsal and middle nasal conchae. Given the high heritage value of the specimens, the transport, handling and storage were done according to Simmons and Muñoz-Saba (2005). A qualitative assessment of the nasal cavity, nasal conchae, and paranasal sinuses was undertaken with special emphasis on the communication between the paranasal sinuses and nasal cavity proper. In addition, an analysis was performed of the surfaces and cavities using helical computed tomography (CT scan; Mx8000 IDT 16, Philips Medical Systems DMC GmbH, Hamburg, Germany). Cross-sectional skull images were acquired in axial exploration mode using parameters according to Brinkschulte et al. (2013): 120 kV, 4100 mAs, image collimation of 1.0 mm, tube rotation time 0.75 s, step (0.438), section thickness 1 mm and a matrix of 999 images. Then the images were reconstructed using a window width of −500 HU (Hounsfield units) and a window level of 2000 HU (kernel smoother). The image analysis was done using the Slicer software version 4.11.2021026 (Fedorov et al., 2012) with the SlicerMorph extension (Rolfe et al., 2021) for DICOM files that enabled the 3D reconstruction. The volumetric and

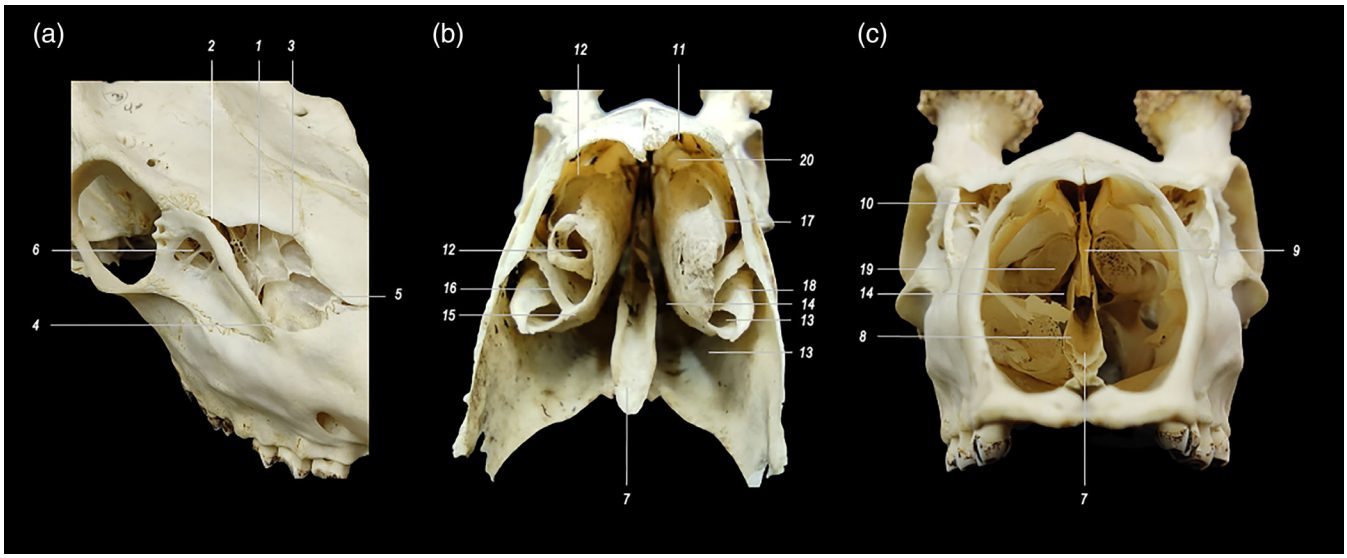

FIGURE 1 Nasal cavity of Patagonian Huemul deer. (a) Left rostrolateral view; (b) rostral view, the incisor bone was disarticulated; (c) rostral view, with bony nasal opening, without ventral and dorsal nasal conchae. 1. nasolacrimal fissure, 2. caudal apex, 3. dorsomedial vertex, 4. ventrolateral vertex, 5. rostral vertex, 6. Fossa lacrimalis externa, 7. septal groove, 8. vomeral crest, 9. perpendicular plate of the ethmoidal bone, 10. Facies nasalis of the lacrimal bone, 11. meatus nasi dorsalis, 12. middle nasal meatus, 13. meatus nasi ventralis, 14. meatus nasi comunis, 15. meatus nasi ventralis, 16. basal plate of ventral nasal concha, 17. dorsal portion of ventral nasal concha, 18. ventral portion of ventral nasal concha, 19. middle nasal concha, 20. dorsal nasal concha.

surface data of the paranasal sinuses were sorted according to age since the factor of ontogeny considerably affects the shape of these structures (e.g., see Ferreira et al., 2021). The linear distances were sorted according to sex for their value in detecting sexual dimorphism in the sinus anatomy (Bangi et al., 2017; ELbaz et al., 2019; Umeres-Alvis, 2019). All quantitative data were ordered using spreadsheet software and expressed as averages and standard deviation. The terminology used throughout this study was based on the (revised) 6th edition of the Nomina Anatomica Veterinaria (NAV) (ICVGAN, 2017).

3 | RESULTS

3.1 | Nasal cavity

The virtual rostral limit was represented by the osseous nasal aperture (*Apertura nasi ossea*) formed by the nasal bone (*Os nasale*) and incisor bone (*Os incisivum*), which formed a small nasoincisive notch (*Nasoincisiva Incisura*) (Figure 1). The caudal limit of the cavity was represented by the choana, comprised of the vomer, pterygoid, basisphenoid, and palatine bones. The ventral wall (floor) was comprised (from rostral to caudal) of the bony palate (*Palatum osseum*), formed by the body and palatine process of the incisive bone (¼ rostral), by the palatine process of the maxilla and by the horizontal plate of the palatine bone (¼ caudal). The nasal crest of both maxillae and the palatine bones formed a groove for the socket of the bony nasal septum. The dorsal wall (roof) was formed by inner side of the nasal bones (rostral) and by the nasal portion of the frontal bone up to the cribriform plate of the ethmoid bone (caudal). The caudal wall was represented by the cribriform plate, which was tilting ventrally toward the body of the presphenoid bone, the region located dorsally to the nasopharyngeal meatus, where the ethmoidal labyrinth is located and limited caudally by the ethmoid bone and was designated inferiorly to the nasal cavity. The medial wall was represented by a bony nasal septum formed by the vomer crest (ventral) and the perpendicular plate of the ethmoid bone (dorsal). It had a staggered dorsal edge, descending caudally, and ending in a round tip. The lateral wall was formed by (rostrally to caudally) the nasal process of the incisive bone (rostral), the nasal side of the body of the maxilla, the nasal side of the lacrimal bone, the perpendicular plate of the palatine bone and the medial side of the pterygoid bone (caudal). At the level of the infraorbital foramen, the opening of the nasolacrimal duct (*Canalis nasolacrimalis*) was observed, which flowed into the ventral nasal meatus (*Meatus nasi ventralis*). The maxillary hiatus, with its convex deltoid shape, was noticeable dorsocaudally to the opening of the nasolacrimal duct. In the region of the maxillary tuber, the sphenopalatine foramen was observed, which communicated with the pterygopalatine fossa.

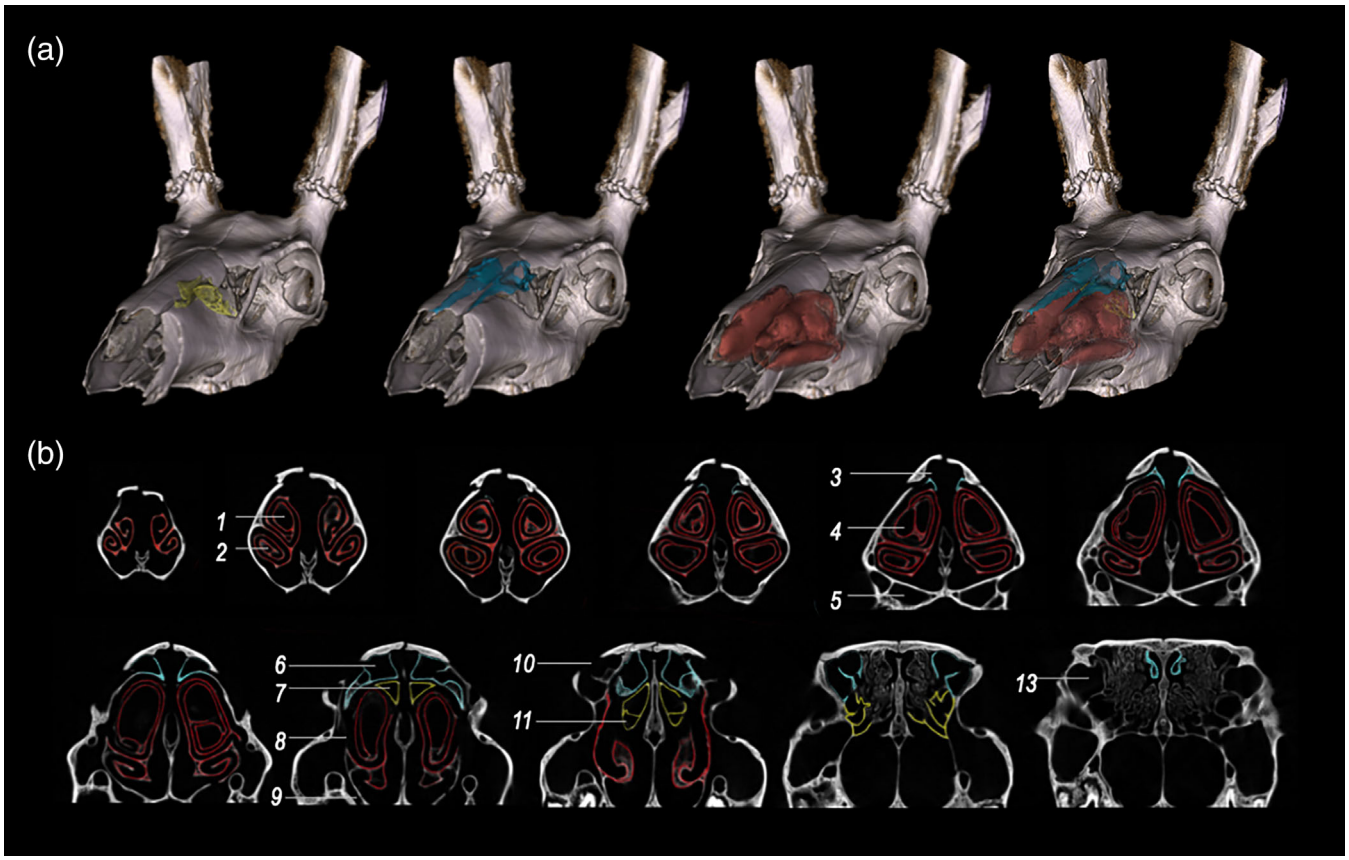

FIGURE 2 3D reconstruction of the Patagonian Huemul deer skull. (a) Right rostrolateral view. Middle nasal concha (yellow), dorsal nasal concha (blue), ventral nasal concha (red); (b) Transverse sections from rostral to caudal; 1. middle nasal meatus, 2. ventral nasal meatus, 3. dorsal nasal meatus, 4. ventral nasal concha bulla, 5. palatine sinus, 6. dorsal conchal sinus, 7. median conchal sinus, 8. nasomaxillary opening, 9. maxillopalatine opening, 10. nasolacrimal fissure, 11. bulla of the middle nasal concha, 12. maxillary sinus, 13. lacrimal sinus, 14. nasopharyngeal meatus.

With respect to the choana, its dorsal wall was represented by the body of the basisphenoid bone. The *medial side* was formed entirely by the pterygoid bone, and the *lateral side* by both the pterygoid process of the basisphenoid bone (dorsal) and by the pterygoid bone (ventral). The medial wall was represented by the caudal projection from the vomer crest.

3.1.1 | Nasolacrimal fissure

This connected with the external side of the skull. It was formed by the nasal, lacrimal, frontal, and maxilla bones and was rhomboid in shape. Its *caudal vertex* was formed between the frontal and lacrimal bones, the *dorsomedial vertex* by the frontal and nasal bones, the *dorsomedial vertex* by the lacrimal and maxilla bones, and the *rostral vertex* by the nasal and maxilla bones. The frontal bone formed its caudodorsal margin, the lacrimal bone the caudoventral margin, the nasal bone the rostrodorsal margin, and the maxilla the rostroventral margin (Figure 1).

3.1.2 | Meatuses

There are six meatuses. The dorsal nasal meatus was between the roof of the nasal cavity and the dorsal nasal concha, the middle nasal meatus between the dorsal nasal concha and the dorsal portion of the ventral nasal concha (at the level of the third premolar, it was divided into a dorsal and ventral projection by the presence of the nasal concha), the ventral nasal meatus between the ventral portion of the ventral nasal concha and the floor of the nasal cavity, the common nasal meatus, medially in the nasal cavity, between the nasal septum and the nasal conchae (extending from the roof to the floor of the nasal cavity, it is medially continuous to the other nasal meatuses), the ethmoidal meatuses, which were formed between the structures of the ethmoidal labyrinth and nasopharyngeal meatus (*Meatus nasopharyngeus*) located between the basal plate of the ethmoid bone (roof) and the floor of the nasal cavity. Their walls were smooth, the roof of the nasopharyngeal meatus projected horizontally, encompassing the basal plate of ethmoid bone and

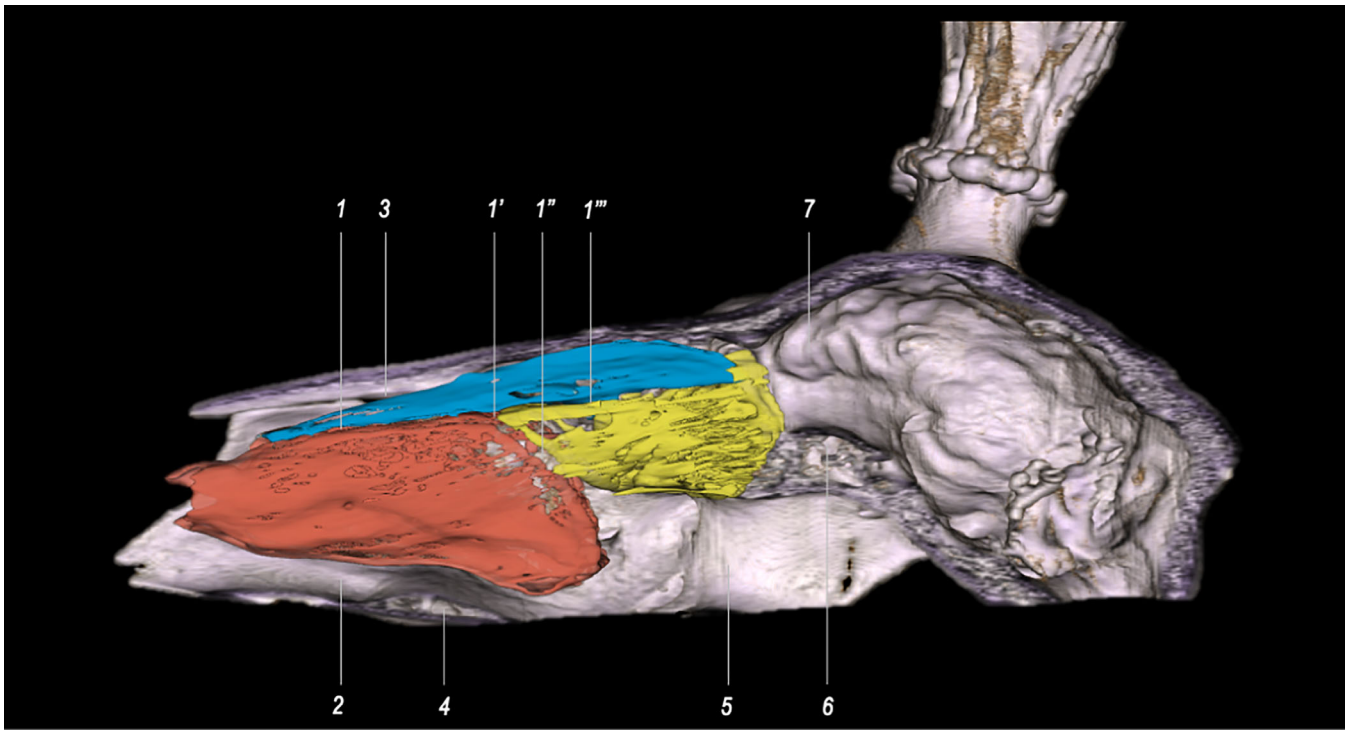

FIGURE 3 3D reconstruction of the Patagonian Huemul deer skull, parasagittal section, medial view. Middle nasal concha (yellow), dorsal nasal concha (blue), ventral nasal concha (red). 1. middle nasal meatus, 1′. bifurcation, 1″. ventral projection, 1‴. dorsal projection, 2. ventral nasal meatus, 4. palatine sinus, 5. nasopharyngeal meatus, 6. sphenoid sinus, 7. cranial cavity.

the body of the presphenoid and basisphenoid bones, with the caudal limit being the choana (Figure 2).

3.2 | Nasal conchae

The Patagonian huemul deer had three nasal conchae: ventral, middle, and dorsal (Figures 2 and 3). In general, the ventral nasal concha was a paired bone that articulated with the nasal side of maxilla, whereas the dorsal and middle nasal conchae were part of the ethmoidal labyrinth. The dorsal and middle nasal conchae corresponded to endoturbinates I and II, respectively, and presented a basal plate from which one or more spiral laminae continued. Along the free margin, bullae were observed, subdivided into cells via the septa. The *ventral nasal concha* extended from the osseous nasal aperture to the level of the interalveolar septum, between the second and third molars. It articulated with the conchal crest of the maxilla by means of a basal plate as its support, in a relatively ventromedial direction (rostral portion). It had a *dorsal portion*, which had medial → dorsal → lateral → ventral winding. Its free margin had rostral and caudal bullae (larger). The dorsal margin ascended slightly caudally until the bifurcation of the middle nasal meatus, from which it tilted ventrally on a 135° angle. The *ventral portion* presented a medial → ventral → lateral → dorsal winding; its free margin presented subdivided bullae. The ventral margin descended caudally, supporting the lateral wall of the nasal cavity in its most caudal portion (Figure 2). The *middle nasal concha* extended from the cribriform plate of the ethmoid bone to the third premolar. Its bone base was comprised of endoturbinate II, ventrally to endoturbinate I. It extended rostrally via a ventral → lateral → dorsal → medial winding, from which the middle conchal sinus was formed (*Sinus conchae mediae*) and a bulla in its rostral portion, with this last one resulting from the formation of a septum by closed winding. The rostral side appeared cribriform. It had a horizontal dorsal margin, whereas the rostral portion of the ventral margin descended and continued with the lateral wall of the nasal cavity (Figure 4).

The *dorsal nasal concha* extended from the cribriform plate of the ethmoid bone to approximately 2 cm before the osseous nasal aperture. Its bone base was formed by endoturbinate I. It had a *rostral portion* with a fine longitudinal projection, suspended and without winding. The caudal portion articulated dorsolaterally with the ethmoidal crest of the nasal bone, coiling longitudinally and laterally, forming the dorsal conchal sinus (*Sinus conchae dorsalis*). The dorsal margin (caudal portion) articulated with the nasal bone (dorsolaterally), whereas the ventral margin descended slightly rostrally.

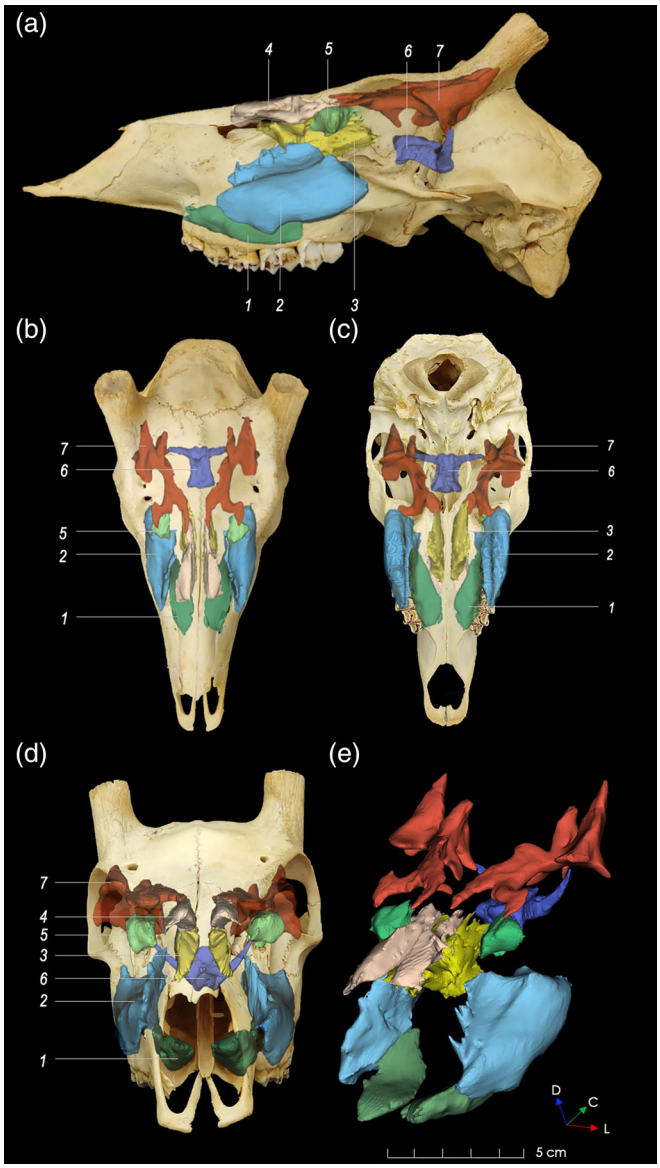

FIGURE 4 3D reconstruction of the paranasal sinuses in the Patagonian Huemul skull. (a) Right side view; (b) dorsal view; (c) ventral view; (d) rostral view; (e) right rostrolateral view of the paranasal sinuses. 1. palatine sinus, 2. maxillary sinus, 3. median conchal sinus, 4. dorsal conchal sinus, 5. lacrimal sinus, 6. sphenoid sinus, 7. frontal sinus.

3.3 | Paranasal sinuses

Generally, it was possible to distinguish two types of sinus systems: the first included the sinuses that communicated collectively with the middle nasal meatus: the maxillary and palatine sinuses; the second included those that communicated directly with the ethmoidal meatuses, on the caudal wall of the nasal cavity: the dorsal conchal, middle conchal, lacrimal, frontal, and sphenoid sinuses (Figure 4). The *dorsal conchal sinus* was paired. It extended from the rostral vertex of the nasolacrimal fissure to the caudal wall of the nasal cavity, located dorsally to the middle conchal sinus. Formed by the dorsal nasal concha (ventromedial wall), by ⅔ rostrally from the inner side of the nasal bone (dorsolateral wall) and by the base of the dorsal nasal concha (caudal wall). It communicated with the nasolacrimal fissure (rostrally) and with the nasal cavity (caudally) via the ethmoidal meatuses. The *middle conchal sinus* was paired and located ventrally to the dorsal conchal sinus. It extended from the bifurcation of the nasal meatus to the caudal wall of the nasal cavity. Its walls were formed by the middle nasal concha. Rostroventrally, there was a bulla formed by a septum. It was wide (dorsally), with concave (laterally and rostrally) and convex walls (medially). It communicated with the nasal cavity (caudally) via the ethmoidal meatuses. The paired maxillary sinus was the most voluminous extending from the region of the infraorbital foramen to the tuberosity of the maxilla. Their walls were formed by the maxilla (rostral, ventral, dorsal, lateral, and caudal walls), zygomatic bone (lateral and caudal walls) and lacrimal bone (caudal, medial, and dorsal walls). Medially and ventrally, it was limited by the infraorbital canal, which was the limit with the palatine sinus (*Sinus palatinus*), sharing the maxillopalatine opening (*Apertura maxillopalatina*). Ventrally it presented a groove formed by the infraorbital canal and dorsally a groove formed by the nasolacrimal duct, and from this it was divided into *ventrolateral* (wide and voluminous) and *dorsomedial* (flattened and thin) portions. It was located laterally and caudally to the palatine sinus, and ventrally to the lacrimal sinus. It shared direct communication to the nasal cavity with the palatine sinus via the nasomaxillary opening formed by the maxillary hiatus, ending at the middle nasal meatus. The *lacrimal sinus* was paired, extended from the interalveolar septum, between the second and third molars, up to the caudal wall of the nasal cavity. Its walls were formed by the lacrimal bone. Pyriform in shape, its vertex presented laterally. It was located dorsally to the caudal limit of the maxillary sinus and ventrally to the rostral limit of the frontal sinus. It communicated directly with the nasal cavity via the ethmoidal meatuses from its caudal wall. The *palatine sinus* was paired and extended from the region of the infraorbital foramen to the interalveolar septum between the second and third molars. Its walls (dorsal, ventral, lateral, medial, rostral, and caudal) were formed by the palatine process of the maxilla. It was limited by the infraorbital canal, sharing the maxillopalatine opening with the maxillary sinus. It was "tongue"-shaped, its ventral and dorsal sides were convex and concave, respectively, ending at the maxillary sinus, via the nasomaxillary opening, in the middle nasal meatus (Figure 4). The *frontal sinus* was paired. It extended from the bottom of the nasal cavity to

the middle of the excrescence of the frontal bone. Its walls (dorsal, ventral, and caudal) were formed by the frontal bone. Rostrally and caudally to the supraorbital foramen were the medial frontal (*Sinus frontalis medialis*) and lateral frontal (*Sinus frontalis lateralis*) sinuses, respectively. The medial frontal sinus was triangular, presenting a base (rostrally) and a vertex oriented toward the lateral frontal sinus. The base provided a separate space, located laterally in the rostral portion, which communicated by small pores with the rest of the medial frontal sinus.

Rostrally, it communicated with the nasal cavity via the frontal sinus openings (*Aperturae sinuum frontalium*) ending at the ethmoidal meatuses. The lateral frontal sinus presented a pyramidal shape with a convex base and close to the orbital side of the frontal bone. Its vertex

TABLE 1 Volume and surface area of paranasal sinuses of the Patagonian huemul deer ($n = 5$).

Sinus		1.5 years	2 years	3 years	4 years	7 years[a]	Average ± SD
Dorsal conchal sinus	cm^3	-	2.95	2.94	5.46	4.77	4.03 ± 1.28
	cm^2	-	24.47	23.58	33.62	28.50	27.54 ± 4.58
Middle conchal sinus	cm^3	-	2.12	3.82	2.57	5.55	3.52 ± 1.54
	cm^2	-	22.59	40.37	16.83	27.68	26.87 ± 10.03
Maxillary sinus	cm^3	16.28	20.98	18.83	32.70	29.65	23.69 ± 7.12
	cm^2	65.13	63.31	61.67	89.28	78.32	71.54 ± 11.9
Lacrimal sinus	cm^3	0.68	1.56	1.65	1.17	1.27	1.27 ± 0.38
	cm^2	6.68	12.31	11.91	9.16	8.51	9.71 ± 2.37
Palatine sinus	cm^3	2.89	5.05	4.07	5.84	7.60	5.09 ± 1.78
	cm^2	25.24	29.42	26.13	33.26	48.19	32.45 ± 9.35
Frontal sinus	cm^3	1.04	2.48	2.53	3.32	2.35	2.34 ± 0.82
	cm^2	36.94	41.99	43.05	38.70	31.10	38.36 ± 4.74
Sphenoidal sinus	cm^3	1.15	2.13	2.63	3.84	1.98	2.35 ± 0.99
	cm^2	19.76	26.53	40.32	30.88	24.94	28.49 ± 7.72

[a]Female.

TABLE 2 Paranasal sinus openings of the Patagonian huemul deer.

Opening	Communication	Observation
Maxillopalatine	Palatine sinus with maxillary sinus	Extended along with the infraorbital canal
Nasomaxillary	Middle nasal meatus with maxillary sinus and via the maxillopalatine opening with the palatine sinus	Convex deltoid shape or inverted arrowhead
Frontosphenoidal[a]	Frontal sinus with sphenoidal sinus	Communication established presenting arc shape, concave rostrally
Openings of the frontal sinus	Medial frontal sinus with ethmoidal meatuses	Located rostroventrally in the medial frontal sinus
Openings of the sphenoidal sinus	Sphenoidal sinus with ethmoidal meatuses	Located in the rostral wall of the sphenoidal sinus
Openings of the lacrimal sinus	Lacrimal sinus with ethmoidal meatuses	Located laterocaudally
Openings of the dorsal conchal sinus	Dorsal conchal sinus with ethmoidal meatuses	Located on the caudal wall of the dorsal conchal sinus
Openings of the middle conchal sinus	Dorsal conchal sinus with ethmoidal meatuses	Located on the caudal wall of the middle conchal sinus

Note: Communications with middle nasal meatus and ethmoidal meatuses are communications with the nasal cavity.
[a]Not included in the NAV.

TABLE 3 Linear distances (average ± SD; mm) of paranasal sinus openings of the Patagonian huemul deer.

Variable	Males ($n = 4$)	Females ($n = 1$)	Total ($n = 5$)
LNM	24.00 ± 1.14	29.00	25.00 ± 2.55
WNM	11.18 ± 0.90	8.00	10.54 ± 1.23
LMP	29.75 ± 5.91	40.00	31.80 ± 6.87
WMP	4.80 ± 1.48	3.90	4.62 ± 1.34
LFO	7.00 ± 2.16	14.00	8.40 ± 3.65
WFO	1.38 ± 0.49	1.90	1.48 ± 0.49
LSO	3.25 ± 1.26	2.00	3.00 ± 1.23
WSO	2.38 ± 0.82	1.50	2.20 ± 0.81
LEM	1.52 ± 0.33	1.34 ± 0.51	1.48 ± 0.30
WEM	2.37 ± 1.58	1.78 ± 0.69	2.25 ± 1.39

Abbreviations: LEM, length ops. ethmoidal meatuses; LFO, length of frontosphenoidal op.; frontal portion; LMP, length maxillopalatine op.; LNM, length nasomaxillary op.; LSO, length of frontosphenoidal op.; sphenoidal portion; WEM, width ops. ethmoidal meatuses; WFO, height of frontosphenoidal op.; frontal portion; WMP, height maxillopalatine op.; WNM, height nasomaxillary op.; WSO, height of frontosphenoidal op.; sphenoidal portion.

was excavated up to the middle of the bony eminences that support the excrescences of the frontal bone. It communicated via small pores that form a caudoventral arc with the lateral portion of the sphenoidal sinus, noting an opening in the frontal sinus and an opening in the sphenoidal sinus for each end of this arc. Cancellous bone tissue was observed in the entire frontal sinus. The *sphenoidal sinus* was the unpaired sinus. It extended from the caudal wall of the nasal cavity to the intersphenoid synchondrosis. Its walls were formed by the presphenoid bone. It presented a central portion, cuboid with four sides, associated with the body of the presphenoid and the optic chiasm. Ventrally, it had two caudal projections that were lateralized and oriented dorsally, excavating the wing of the presphenoid bone. The caudal side presented a notch between the caudal projections. The dorsal side presented a smooth surface, tilted slightly caudally. The lateral side was concave. The rostral side presented a communication with the nasal cavity, the opening of the sphenoid sinus (*Apertura sinus sphenoidalis*), ending at the ethmoidal meatuses. Table 1 provides the volume and surface area of the paranasal sinuses. Table 2 presents the communications between paranasal sinuses and openings to the nasal cavity. Table 3 presents the linear distances (length and width) of the nasomaxillary opening (LNM and WNM), maxillopalatine opening (LMP and WMP), opening of the frontal sinus (LFO and WFO), opening of the sphenoid sinus (LSO and WSO), and openings of the paranasal sinuses toward the ethmoidal meatuses (LEM and WEM).

4 | DISCUSSION

Here we provide, to the best of our knowledge, the first osteological description of the nasal cavity (with emphasis on the nasoturbinal and maxilloturbinal regions), paranasal sinuses and nasal conchae in skulls of the endangered Patagonian huemul deer obtained from several sites in Chile and based on an approach limited by the preservation of the skulls, the quality of the CT images obtained, and the three-dimensional reconstruction. Using semiautomatic segmentation, we reconstructed in 3D all the sinus and nasal conchae compartments and described not only the individual structures, but also the sinonasal communication channels. The CT with three-dimensional reconstruction of skulls proved to be a valuable and useful method. Equally, it has become an important method not only for the diagnosis of diseases of the paranasal sinuses, but also during the anatomical description of endangered wild animals of high cultural value. The correct visualization, identification and demarcation of the nasal conchae and paranasal sinuses were challenging due to their complex anatomy. The openings that connected different sinuses were present in each skull studied and were clearly identifiable. The determination of the borders of the paranasal sinuses and their communications tested the experience of the examiner. The identification of the sinonasal communication channels (openings) and the techniques used have been widely described in domestic animals of the same body contexture and condition (Köhler et al., 2021). A relevant aspect is that, since we studied skulls, there were no surrounding structures (mucosa, soft tissue, etc.), and thus it was possible to take a reliable measurement. The *postmortem* changes and mainly the absence of soft tissue provided a better view of the walls and bony septa. The swelling of the mucosa during anesthesia and the partial volume effect are reported hazards (Stieger-Vanegas & Hanna, 2022) that could affect the presentation and evaluation of the sinonasal communication channels in *in vivo* assessments on anaesthetized animals. A macroscopic study of head dissection would be useful to clarify, compare, and complement the background of communication and sinus volumetry. Although we discussed and compared the bone findings observed in the Patagonian huemul deer with domestic animals, we did so from a morphological perspective considering that they are animals of a similar body size and in no case from an ecological or evolutionary perspective. Given that the shape of the cranium and

facies varies among species, these data will (i) facilitate the identification of skulls and/or species in paleontological studies based on structural and geographic criteria, (ii) improve the criteria and surgical approaches of the skull, and in particular (iii) improve the historical, ecological, and evolutionary understanding of the Patagonian huemul deer.

4.1 | Regarding the anatomy of the nasal cavity, nasal conchae, and paranasal sinuses

The osseous nasal aperture contained a nasoincisive notch similar to the description in roe deer (*Capreolus capreolus*; Onuk et al., 2013), red deer (*Cervus elaphus*; Castaños, 2017), pudu (*Pudu puda*; Saldivia & Villegas, 2019), and taruca (*Hippocamelus antisensis*; Coacalla et al., 2021). A phylogenetic consequence could account for what was observed in the Patagonian huemul deer in terms of the bones that form the nasoincisive notch (Clifford & Witmer, 2005). Some small ruminants that share habitat with the huemul deer such as the goat (*Capra aegagrus hircus*) and sheep (*Ovis orientalis aries*) present a nasal aperture made up of nasal, incisive and maxillary bones (Nickel et al., 1984). In the case of wild cervids, the nasal aperture of the moose is formed by the nasal bone and maxilla, in the case of the reindeer it is formed by an accessory bone to the maxilla (Clifford & Witmer, 2005; reindeer; *Rangifer tarandus*; Castaños, 2017). In these last species, the adaptive traits could play a role. For example, the moose has an extremely large bony nasal aperture oriented obliquely, likely due to its expanded proboscis and nasal vestibule, with its nose being different from all the other cervids. These attributes suggest a mechanical function that provides for an elaborate system for closing the nostrils, probably due to their particular semiaquatic behavior (Clifford & Witmer, 2005; Márquez et al., 2019). The Patagonian huemul deer, being a terrestrial cervid, this mechanical function would not determine the shape of the nasal cavity, thus its nasal opening is oriented on the horizontal axis in such a way that it takes advantage of a greater extension of the nasal cavity and particularly the bony component. The latter has been declared an ancestral cervid condition (Márquez et al., 2019).

In the Patagonian huemul deer, the margin of the lateral wall of the choana differs from the pudu and roe deer. In the first, the choana connects the pterygoid and basisphenoid bones since the perpendicular plate of the palatine bone is not part of the choana margin. However, in the pudu and roe deer, the margin of this wall is connected to the palatine bone (Onuk et al., 2013; Saldivia & Villegas, 2019). Since they share habitat, this information is useful for differentiating the Patagonian huemul deer from the pudu and the roe deer starting from the skeleton; therefore, these findings are another criterion to consider in zooarchaeological practices.

The presence of a nasolacrimal fissure, typical of cervids, appears in the Patagonian huemul deer. Although George (2001) indicated that in ruminants this fissure is covered only by skin, studies on the roe deer and taruca have demonstrated that it is covered by a cartilage (Coacalla et al., 2021; Onuk et al., 2013). Given the phylogenetic proximity with the taruca, it may be suggested that the Patagonian huemul deer also presents a cartilage over this space.

The nasal conchae were similar to what has been described in goats (Nickel et al., 1979), except in the case of middle nasal concha of the huemul deer, which presented a single spiral lamina and not a double as has been reported in goats, sheep, and bovines (Nickel et al., 1979). There are little or no detailed anatomical descriptions of the nasal conchae in cervids that share habitats with huemul deer (e.g., taruca and pudu; Onuk et al., 2013; Saldivia & Villegas, 2019), which means a trait conserved in cervids cannot be determined. In the case of the moose, like the osseous nasal aperture, the anatomy of its nasal conchae differs from that of the Patagonian huemul deer, because they are retracted and small given the development of the nasal vestibule (Clifford & Witmer, 2005). Considering these aspects, it may be assumed that the anatomy of the nasal complex of the Patagonian huemul deer is inherent to a terrestrial cervid, since that of the moose favors the semiaquatic life over the extension of different nasal conchae.

The bottom of the nasal cavity revealed narrow ethmoidal labyrinths similar to those reported in the white-tailed deer (Ranslow et al., 2014) and the domestic dog (Craven et al., 2010). This suggests that the Patagonian huemul deer could develop unique nasal air flow patterns when smelling, optimized for the delivery of odorants and characterized by a unidirectional air flow at the bottom of the nasal cavity with a period of stagnation when exhaling. The numerous ethmoidal meatuses observed in the Patagonian huemul deer could contribute to the deposition of odorants by increasing the surface available for chemical detection (Ranslow et al., 2014).

4.2 | Morphofunctional aspects of the paranasal sinuses

In particular, the absence of the ventral conchal sinus in the nasal cavity of the Patagonian huemul deer has morphofunctional implications, such as: greater speed of air

flow and lower capacity for air to maintaining heat and water balance (Zárate, 2014). The latter could be compensated by the extension observed in the ventral nasal concha by occupying almost 50% of the length of the nasal cavity, the requirements of warming and moisture through its length rather than its branching (Ranslow et al., 2014). The communications observed between frontal and sphenoid sinuses (via a frontosphenoidal opening) and between the second sinus system and the ethmoidal meatuses (where there is usually olfactory mucosa) may have an explanation in the need to reinforce the olfactory and reproductive functions (Zárate, 2014).

The cancellous bone formation of the frontal bone and the presence of bony septa in the frontal sinus demonstrate the properties of the skull to resist multidirectional forces when dissipating the energy in large areas (Márquez, 2008), which could be a consequence of the ecological needs associated with the mechanical impacts on their heads (Núñez-Cook et al., 2022) and not only olfactory needs (Zárate, 2014). In addition, the extension of the frontal sinus within the pedicles—the cylindrical excrescences of the frontal bone—possibly suggests their function in absorbing and releasing mechanical energy, as has been described in the goat (Alsafy et al., 2021). This function of mechanical dissipation by the frontal sinus is usually greater in skulls with a convex frontal bone (Curtis et al., 2015), as reported in the Patagonian huemul deer (Núñez-Cook et al., 2022).

Apparently, the presence of a maxillary sinus is a shared primitive characteristic among placental mammals. In cervids, the literature describes differences in their shape and size; for example, the presence of an incomplete septum that subdivides the maxillary sinus in the Indian muntjac (*Muntiacus muntjak*) and the sambar (*Rusa unicolor*; Keneisenuo et al., 2022), a trait not observed in the Patagonian huemul deer or in the white-tailed deer (Márquez et al., 2019). The roe deer and the red deer do not have a frontal sinus (Pohlmeyer, 1977, 1978), which the Patagonian huemul deer, the muntjac and the sambar do. The pneumatization of the palate, represented by the presence of a palatine sinus, is a relevant finding in the Patagonian huemul deer. This characteristic is shared with the moose (*Alces alces*)—a cervid with semiaquatic behavior with an extreme pneumatization—and with the white-tailed deer (*Odocoileus virginianus*; Márquez et al., 2019), but not with the muntjac and the sambar. It is known that pneumatization of the bones fulfills a role in reducing the weight of the skull (Nickel et al., 1979), or it is a site of passage for vascular structures (Blanco Sucino, 2013). Consequently, the anatomy of the paranasal sinuses of the Patagonian huemul deer presents similarities and differences with some previously mentioned cervids, which corroborates the importance of treating the *nasal complex* as a functional unit integrated by several structures that may be individually subject to selection at different speeds and magnitudes as a result of the diversity of ecological stimuli toward a certain population, as well as due to climatic factors, interspecific and intraspecific interactions, and others (Márquez & Laitman, 2008). For example, in primates environmental conditions reportedly have an effect on the morphometrics of the paranasal sinuses, tending to reduce the sinus volume in colder atmospheres (Márquez & Laitman, 2008; Rae et al., 2003); therefore, assuming the same happens in the Patagonian huemul deer, the volumetric data collected in this work will facilitate comparative studies between phylogenetically close cervid species in warmer atmospheres (like the taruca; *Hippocamelus antisensis*), obtaining proportional differences.

4.3 | Clinical-surgical implications of the paranasal sinuses

The nasal cavity is the main access for pathogens to the respiratory system. Considering the two sinus systems observed in the Patagonian huemul deer and given the presence of the maxillopalatine and nasomaxillary openings, the maxillary and palatine sinuses are at greater risk of bacterial infection and consequently of a clinical presentation of sinusitis. This would involve surgical fenestrations in the maxillary sinus as the treatment for sinusitis (Boiani Fernández & Van Wassenhove Olascoaga, 2015), having an impact on the first sinus system (maxillary and palatine sinuses) and not on the rest of the sinuses. Pathologies associated with these systems such as paranasal sinus hypoplasia, atelectasis and sinusitis may be interpreted by using the normal volumetric properties of the paranasal sinuses as a reference (Wang et al., 2021).

In terms of the volume of the paranasal sinuses and their relation to age, the findings suggest certain growth periods in the Patagonian huemul deer, given the difference in volumes observed in skulls of different ages (Ferreira et al., 2021; Rossie, 2006; Spaeth et al., 1997). In this respect, a greater volume of the frontal sinus has been observed in large animals, which has been associated with a useful mechanism to lighten the load. Our volumetric data in males suggest an association between the increase in the total volume of the frontal sinus and the passage of time (age), assuming that this phenomenon is related to body growth. Previously, we have reported evidence of the likely detrimental effect on bone quality (Núñez-Cook et al., 2022) induced by chronic

metabolic imbalances as a response to the mineral deficiency reported in the huemul deer (Flueck, 2018). Therefore, the volumetric data reported in the present study are relevant from a conservation perspective, since osteopathies and secondary infections (like sinusitis) could explain the limited ability of the Patagonian huemul deer to avoid predators and optimize the development of its ecology and, therefore, explain the population's lack of recovery (Flueck, 2018; Flueck & Smith-Flueck, 2017).

Knowledge of the anatomy and morphometrics of the openings of the paranasal sinuses has been considered relevant given the high prevalence of sinusitis (Brinkschulte et al., 2014). It is suspected that the obstruction of the sinus openings is a primary factor in its etiopathogeny, with this depending on factors such as the quality and resorption of mucus, the activity of the cilia, as well as the inflammation of the mucosa that consequently occludes the sinus opening, thereby preventing its drainage (Brinkschulte et al., 2014). For example, in horses a hyperplasia of the paranasal sinus mucosa of up to 15 mm has been described (Tremaine et al., 1999). This highlights the need to know about linear morphometric data in the Patagonian huemul deer and other dolichocephalous wild animal in cases of (i) imaging exploration of sinuses during the clinical examination to assess and rule out probable occlusions of openings and (ii) when performing minimally invasive procedures like functional endoscopic surgery of the paranasal sinuses to restore sinus drainage and ventilation in the openings (Kennedy, 2006). Finally, the differences observed between male and female skulls in the linear measurements of the nasomaxillary, nasopalatine and frontosphenoidal openings suggest a sexual dimorphism, although more studies are needed in this regard, and it is an important aspect to consider in surgical procedures.

4.4 | Limitations of the study

The study of paranasal sinuses and their communications via sagittal dissection of biological samples could lead to errors given that the sinus openings were close to the midline, possibly being obliterated by the saw, whereas those located peripherally tend to be more hidden, which leads to the complete dissection of the skull being a partial solution (Rossie, 2006). Research initiatives have been hampered by the necessary destruction of the anatomical sample obtained by dissection in sufficiently large species and in particular in species with a high cultural value as in the case of the Patagonian huemul deer. Thus, CT has been implemented as a noninvasive and nondestructive means to view the paranasal anatomy (Rossie, 2006). The 3D reconstruction from CT was very useful for the visualization of the spatial shape of the nasal complex, and in the facilitation of the exchange of information of the species in libraries or digital museums. One limitation identified regarding the 3D reconstruction was the weak marking of some fibrous joints, which made it difficult to delimit some bones and their structures. The same difficulty was observed in the identification of some foramina and communications between sinuses due to the shading of the images. The information studied made it possible to state that the morphology of the paranasal sinuses and nasal conchae is compatible with the ecology and phylogeny of the species, and can be compared with animals of similar habits and close relatives. During the identification and observation of complete skulls, the tomographic images were complementary; therefore, the findings described in the present study offer a high potential to argue for further research on wild animals, and to be used as a reference in the surgical clinical routine of the endangered Patagonian huemul deer.

In conclusion, the Patagonian huemul presents a wide, large nasal cavity, with a bony nasal opening typical of cervids and a choana with characteristics that differentiate it from the pudu and roe deer. In addition, it has six nasal meatuses and three nasal conchae, with the ventral nasal concha having the greatest volume and surface, which, given its extension, ensures a greater ability to humidify and heat the air. There is also, a complex

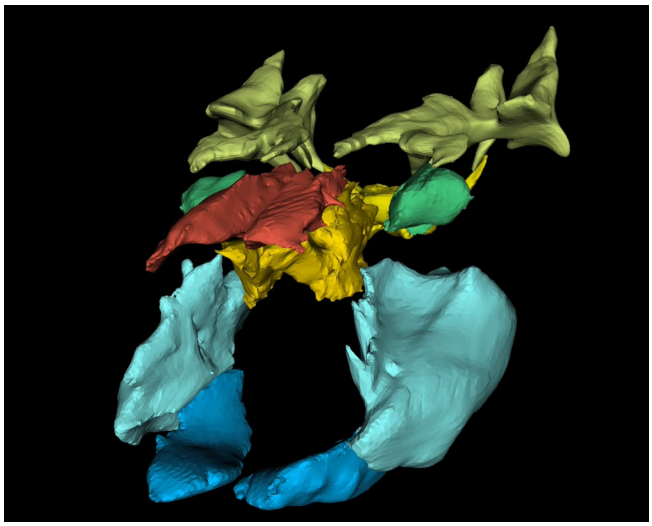

VIDEO 1 3D Reconstruction of the paranasal sinuses in endangered Patagonian huemul deer. Blue: Palatine sinus; Light blue: Maxillary sinus; Dark green: Lacrimal sinus; Light green: Frontal sinus; Red: Dorsal conchal sinus; Dark yellow: Middle conchal sinus; Light yellow: Sphenoidal sinus.
Video content can be viewed at https://onlinelibrary.wiley.com/doi/10.1002/ar.25230

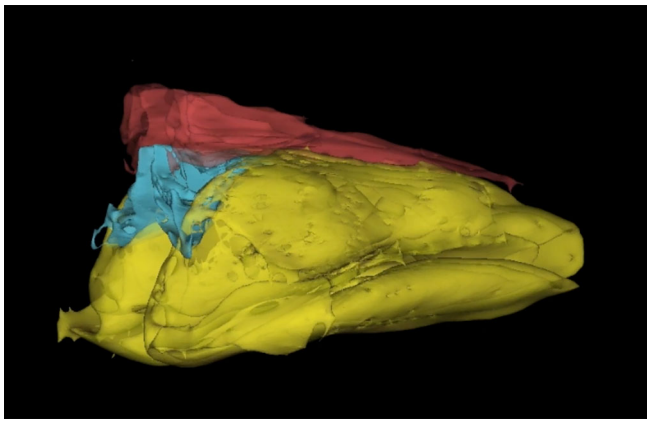

VIDEO 2 3D Reconstruction of the nasal conchae in endangered Patagonian huemul deer. Red: Dorsal nasal concha; Blue: Middle nasal concha; Yellow: Ventral nasal concha. Video content can be viewed at https://onlinelibrary.wiley.com/doi/10.1002/ar.25230

system of paranasal sinuses characterized by a rostroventral and interconnected group, where communication with the nasal cavity via the nasomaxillary opening is common, and a caudodorsal group that communicates with the nasal cavity through openings in the nasal meatuses (Videos 1 and 2).

AUTHOR CONTRIBUTIONS

Samuel Núñez-Cook: Investigation; writing – original draft; writing – review and editing; methodology; formal analysis; software. **Fernando Vidal-Mugica:** Resources; investigation; writing – original draft; writing – review and editing. **Paulo Salinas:** Conceptualization; investigation; funding acquisition; writing – review and editing; writing – original draft; supervision; methodology; formal analysis; software; resources.

ACKNOWLEDGMENTS

The authors acknowledge the support of PUCV-DI 039.407/2021 (Paulo Salinas) Innovative Interdisciplinary Research.

FUNDING INFORMATION

No funds, grants, or other support was received.

CONFLICT OF INTEREST STATEMENT

The authors declare no conflicts of interest.

ORCID

Samuel Núñez-Cook https://orcid.org/0000-0003-3778-6812

Paulo Salinas https://orcid.org/0000-0003-2273-0904

REFERENCES

Alsafy, M., Madkour, N., Abumandour, M., El-Gendy, S., & Karkoura, A. (2021). Anatomical description of the head in Ossimi Sheep: Sectional anatomy and computed tomographic approach. *Morphologie*, *105*(348), 29–44.

Bangi, B. B., Ginjupally, U., Nadendla, L. K., & Vadla, B. (2017). 3D evaluation of maxillary sinus using computed tomography: A sexual dimorphic study. *International Journal of Dentistry*, *2017*, 9017078.

Blanco Sucino, D. (2013). *Aportaciones al conocimiento anatómico de la cabeza en el dromedario (Camelus dromedarius L.) mediante tomografía computerizada y cortes macroscópicos*. Ph.D. Thesis, Universidad de Las Palmas de Gran Canaria, Las Palmas de Canaria, España.

Boiani Fernández, M. V., & Van Wassenhove Olascoaga, M. C. (2015). Manejo y resolución de un caso clínico de sinusitis crónica en equinos. Ph.D. Thesis, Universidad de la República, Montevideo, Uruguay.

Brinkschulte, M., Bienert-Zeit, A., Lüpke, M., Hellige, M., Ohnesorge, B., & Staszyk, C. (2014). The sinonasal communication in the horse: examinations using computerized three-dimensional reformatted renderings of computed-tomography datasets. *BMC Veterinary Research*, *10*(1), 1–10.

Brinkschulte, M., Bienert-Zeit, A., Lüpke, M., Hellige, M., Staszyk, C., & Ohnesorge, B. (2013). Using semi-automated segmentation of computed tomography datasets for three-dimensional visualization and volume measurements of equine paranasal sinuses. *Veterinary Radiology & Ultrasound*, *54*(6), 582–590.

Castaños, J. (2017). *Grandes faunas esteparias del Cantábrico oriental estudio isotópico y paleontológico de los macrovertebrados del pleistoceno superior de kiputz ix (mutriku, gipuzkoa)* (1st ed., p. 218). KOBIE.

Clifford, A. B., & Witmer, L. M. (2005). Case studies in novel narial anatomy: 2. The enigmatic nose of moose (Artiodactyla: Cervidae: *Alces alces*). *Journal of Zoology*, *262*(4), 339–360.

Coacalla, C. Z., Curie, J. I. P., & Flores, J. C. A. (2021). Descripción osteológica de la taruca (*Hipocamelus antisensis*) (d'Orbigny, 1834): II. Esqueleto axial. *Revista de Investigaciones Veterinarias del Perú*, *32*(6), e21703.

Craven, B. A., Paterson, E. G., & Settles, G. S. (2010). The fluid dynamics of canine olfaction: unique nasal airflow patterns as an explanation of macrosmia. *Journal of the Royal Society Interface*, *7*, 933–943.

Curtis, A. A., Lai, G., Wei, F., & Van Valkenburgh, B. (2015). Repeated loss of frontal sinuses in arctoid carnivorans. *Journal of Morphology*, *276*(1), 22–32.

ELbaz, D. A., El-Shall, O., & El Kolaly, H. (2019). Sexual dimorphism by analysis of maxillary sinus dimensions in a sample of Egyptian population using cone beam computed tomography. *Al-Azhar Dental Journal for Girls*, *6*(4), 385–390.

Escobar Ruíz, M., Smith, J. M., & Flueck, W. T. (2020). *El Huemul: Shoonem, Madera que se mueve/re...* (2nd ed., p. 108). Biblioteca Popular "Dr. Enrique Perea".

Fatterpekar, G. M., Delman, B. N., & Som, P. M. (2008). Imaging the paranasal sinuses: where we are and where we are going. *Anatomical Record (Hoboken)*, *291*(11), 1564–1572.

Fedorov, A., Beichel, R., Kalpathy-Cramer, J., Finet, J., Fillion-Robin, J. C., Pujol, S., Bauer, C., Jennings, D., Fennessy, F.,

Sonka, M., Buatti, J., Aylward, S. R., Miller, J. V., Pieper, S., & Kikinis, R. (2012). 3D Slicer as an image computing platform for the quantitative imaging network. *Magnetic resonance imaging*, *30*(9), 1323–1341.

Ferreira, J. D., Dozo, M. T., de Moura Bubadué, J., & Kerber, L. (2021). Morphology and postnatal ontogeny of the cranial endocast and paranasal sinuses of capybara (*Hydrochoerus hydrochaeris*), the largest living rodent. *Journal of Morphology*, *283*(x1), 66–90.

Flueck, W. T. (2015). Osteopathology and selenium deficiency co-occurring in a population of endangered Patagonian huemul (*Hippocamelus bisulcus*). *BMC Research Notes*, *8*(1), 330.

Flueck, W. T. (2018). Elusive cranial lesions severely afflicting young endangered Patagonian huemul deer: A case report. *BMC Research Notes*, *11*(1), 638.

Flueck, W. T. (2020). Nutrition as an etiological factor causing diseases in endangered huemul deer. *BMC Research Notes*, *13*(276), 1–12.

Flueck, W. T., & Smith-Flueck, J. M. (2017). Troubling disease syndrome in endangered live Patagonian huemul deer (*Hippocamelus bisulcus*) from the Protected Park Shoonem: Unusually high prevalence of osteopathology. *BMC Research Notes*, *10*, 739.

Flueck, W. T., & Smith-Flueck, J. M. (2020). The next frontier for recovering endangered huemul (*Hippocamelus bisulcus*): How to avoid recurrent misdiagnoses of health status and risks. *Animal Production Science*, *60*(10), 1271.

George, M. (2001). *Guide to regional ruminant anatomy based on the dissection of the goat "The Skeleton"* (1st ed., p. 243). Lowa State University Press.

Hofmann, R. R. (1989). Evolutionary steps of ecophysiological adaptation and diversification of ruminants: a comparative view of their digestive system. *Oecologia*, *78*, 443–457.

International Committee on Veterinary Gross Anatomical Nomenclature (ICVGAN). (2017). *Nomina Anatomica Veterinaria* (6th ed., p. 178). Editorial Committee Hanover, Germany.

Keneisenuo, K., Choudhary, O. P., Kalita, P. C., Duro, S., Kalita, A., Doley, P. J., Arya, R. S., Debroy, S., & Priyanka, P. (2022). A comparative study on the morphology, radiography and computed tomography of the skull bones of barking deer (Muntiacus muntjak) and sambar deer (Rusa unicolor). *Folia Morphologica*, *81*(1), 164–174.

Kennedy, D. W. (2006). Technical innovations and the evolution of endoscopic sinus surgery. *The Annals of Otology, Rhinology, and Laryngology. Supplement*, *196*, 3–12.

Köhler, L., Schulz-Kornas, E., Vervuert, I., Gittel, C., Winter, K., Berner, D., & Gerlach, K. (2021). Volumetric measurements of paranasal sinuses and examination of sinonasal communication in healthy Shetland ponies: anatomical and morphometric characteristics using computed tomography. *BMC Veterinary Research*, *17*(1), 41.

Llanos-Soto, S., González-Muñoz, P., Opazo-Capurro, A., González-Rocha, G., & González-Acuña, D. (2020). Subcutaneous abscess caused by Trueperella pyogenes in a Southern pudu (*Pudu puda*). *Austral Journal of Veterinary Sciences*, *52*(2), 67–69.

Márquez, S. (2008). The paranasal sinuses: The last frontier in craniofacial biology. *Anatomical Record*, *291*, 1350–1361.

Márquez, S., & Laitman, J. T. (2008). Climatic effects on the nasal complex: A CT imaging, comparative anatomical, and morphometric investigation of *Macaca mulatta* and *Macaca fascicularis*. *Anatomical Record*, *291*, 1420–1445.

Márquez, S., Pagano, A. S., Mongle, C. S., Albertine, K. H., & Laitman, J. T. (2019). The nasal complex of a semiaquatic artiodactyl, the moose (*Alces alces*): Is it a good evolutionary model for the ancestors of cetaceans? *Anatomical Record*, *302*(5), 667–692.

Nickel, R., Schummer, A., Seiferle, E., Frewein, J., Wille, K. H., & Wilkens, H. (1984). *Lehrbuch der anatomie der haustiere I: Bewegungs apparat* (5th ed., p. 543). Verlag Paul Parey.

Nickel, R., Schummer, A., Seiferle, E., & Sack, W. O. (1979). *The viscera of the domestic mammals* (2nd ed., p. 430). Springer.

Núñez-Cook, S., Vidal Mugica, F., & Salinas, P. (2022). Skull anatomy of the endangered Patagonian huemul deer (*Hippocamelus bisulcus*). *Anatomia, Histologia, Embryologia*, *51*(6), 728–739.

Onuk, B., Kabak, M., & Atalar, K. (2013). Anatomic and craniometric factors in differentiating roe deer (*Capreolus capreolus*) from sheep (*Ovis aries*) and goat (*Capra hircus*) skulls. *Archives of Biological Sciences*, *65*(1), 133–141.

Pohlmeyer, K. (1977). Nasal cavity and paranasal sinuses of the roe-deer (*Capreolus capreolus*) (corrision-anatomical and x-ray studies). *Gegenbaurs morphologisches Jahrbuch*, *123*(5), 708–726.

Pohlmeyer, K. (1978). The nasal cavity and paranasal sinuses of the red deer (*Cervus elaphus*)-anatomical corrosion studies. *Gegenbaurs morphologisches Jahrbuch*, *124*(2), 215–229.

Rae, T. C., Hill, R. A., Hamda, Y., & Koppe, T. (2003). Clinal variation of maxillary sinus volume in Japanese macaques (*Macaca fuscata*). *American Journal of Primatology*, *59*, 153–158.

Ranslow, A. N., Richter, J. P., Neuberger, T., Van Valkenburgh, B., Rumple, C. R., Quigley, A. P., Pang, B., Krane, M. H., & Craven, B. A. (2014). Reconstruction and morphometric analysis of the nasal airway of the white-tailed deer (*Odocoileus virginianus*) and implications regarding respiratory and olfactory airflow. *Anatomical Record*, *297*, 2138–2147.

Rolfe, S., Pieper, S., Porto, A., Diamond, K., Winchester, J., Shan, S., Kirveslahti, H., Boyer, D., Summers, A., & Maga, A. M. (2021). SlicerMorph: An open and extensible platform to retrieve, visualize and analyse 3D morphology. *Methods in Ecology and Evolution*, *12*(10), 1816–1825.

Rossie, J. B. (2006). Ontogeny and homology of the paranasal sinuses in Platyrrhini (Mammalia: Primates). *Journal of Morphology*, *267*(1), 1–40.

Saldivia, M., & Villegas, F. (2019). Descripción anatómica de los segmentos óseos que componen el cráneo de la especie *Pudu puda*. *International Journal of Morphology*, *37*(1), 167–173.

Salinas, P., Arenas-Caro, A., Núñez-Cook, S., Moreno, L., Curihuentro, E., & Vidal, F. (2020). Morphometric, anatomic and radiographic study of bone of the pelvic limb of endangered Patagonian Huemul Deer (*Hippocamelus bisulcus*). *International Journal of Morphology*, *38*(3), 747–754.

Salinas, P., Núñez-Cook, S., Arenas-Caro, A., Moreno, L., Curihuentro, E., & Vidal, F. (2020). Anatomy, morphometry and radiography in the thoracic limb bones of the Patagonian Huemul Deer (*Hippocamelus bisulcus*). *Anatomia, Histologia, Embryologia*, *49*(4), 494–501.

Simmons, J. E., & Muñoz-Saba. (2005). *CONSERVACIÓN INTERNACIONAL serie manuales para la conservación I: Cuidado,*

manejo y conservación de las colecciones biológicas (1st ed., p. 146). Universidad Nacional de Colombia.

Spaeth, J., Krügelstein, U., & Schlöndorff, G. (1997). The paranasal sinuses in CT-imaging: development from birth to age 25. *International Journal of Pediatric Otorhinolaryngology*, *39*(1), 25–40.

Stieger-Vanegas, S. M., & Hanna, A. L. (2022). The role of computed tomography in imaging non-neurologic disorders of the head in equine patients. *Frontiers in Veterinary Science*, *9*, 798216.

Tremaine, W. H., Clarke, C. J., & Dixon, P. M. (1999). Histopathological findings in equine sinonasal disorders. *Equine Veterinary Journal*, *31*, 296–303.

Umeres-Alvis, M. (2019). Morfometría del seno maxilar para estimar el sexo. *Revista Científica Odontológica (Lima)*, *7*(1), 23–33.

Wang, X., Liu, A., Zhao, J., Elshaer, F. M., & Massoud, D. (2021). Anatomy of the Skull of Saanen Goat. An anesthesiology and stereology approach. *International Journal of Morphology*, *39*(2), 423–429.

Zárate, R. (2014). Caracterización anatómica de los senos paranasales de la alpaca (*Vicugna pacos*). Thesis, Universidad Nacional Mayor de San Marcos, Lima.

How to cite this article: Núñez-Cook, S., Vidal-Mugica, F., & Salinas, P. (2024). Anatomy and computed tomography of the nasal cavity, nasal conchae, and paranasal sinuses of the endangered Patagonian huemul deer (*Hippocamelus bisulcus*). *The Anatomical Record*, *307*(1), 141–154. https://doi.org/10.1002/ar.25230